Technical Notes

Rotational Waves in the Plume of an Externally-Mounted Hall Thruster Cathode

Shadrach T. Hepner,* Edward Tang,† Ethan T. Dale,‡ and Benjamin A. Jorns§
University of Michigan, Ann Arbor, Michigan 48109

https://doi.org/10.2514/1.J060578

Introduction

THE hollow cathode is the electron source most commonly employed for Hall effect thrusters (HETs). The electrons emitted by these devices serve the dual roles of impact ionizing the HET propellant and neutralizing it once it has been accelerated (Fig. 1). The electrical coupling from the cathode to the HET discharge is thus a critical driver for their efficient operation. In light of this fact, there have been a number of efforts to characterize the local processes governing the cathode-to-main discharge environment. These studies have revealed that this region is nonclassical and characterized by a wide range of instabilities that can influence the electrical coupling [1–7]. In particular, for thrusters with centrally mounted cathodes (i.e., concentric with the main discharge), there is a large-amplitude "antidrift" azimuthal mode in the cathode plume [1] that may dominate the local electrical coupling [8].

With that said, all HETs that have been flown to date employ *externally mounted* cathodes, i.e., configurations where the electron source is mounted outside the main discharge (Fig. 1). It has yet to be seen if the antidrift instability persists for this more common thruster type. This is a pressing question given the potentially dominant impact the wave may have on the near-field dynamics. With this in mind, this Note presents the first experimental attempt to identify if the same type of rotational wave that has been observed for HETs with centrally mounted cathodes persists for a thruster with an external cathode. We describe in the following the experimental procedure used to search for these waves (Sec. II), the results of this analysis with discussion of the findings (Secs. III and IV), and the major conclusions (Sec. V).

II. Experimental Procedure

We performed this investigation on the H9, which is a 9-kW-class magnetically shielded Hall thruster developed by the University of Michigan, NASA's Jet Propulsion Laboratory, and the U.S. Air Force Research Laboratory [9,10]. This thruster's baseline configuration employs a centrally mounted cathode that exhibits a strong antidrift wave [8]. To investigate the role of location on the formation of this wave for this study, we moved the cathode to a point outside the main discharge (Fig. 1). As in a previous cathode study by Jorns et al. [8], we operated the thruster at 300 V and 15 A with a 7% cathode flow fraction and with the thruster body electrically tied to the cathode [11]. Tests were performed in the Large Vacuum Test Facility at the University of Michigan, which is a 9-m-long 6-m-diameter cryogenically pumped vacuum chamber. The facility background pressure during testing was 6 μtorr, as measured by a Stabil ion gauge oriented downstream and placed 1 m from the thruster in its exit plane [11,12].

We used a Photron Fastcam SA5, which is a high-speed camera, to image oscillations across the face of the thruster at a frame rate of 300 kfps, measuring a total of 50,000 frames. Figure 2 shows a single still frame from the camera, where the cathode and a portion of the thruster channel are visible. For this analysis, we only focused on the highlighted region of Fig. 2, which consists of 40×40 pixels. To relate measurements of plasma luminosity to assessments of variations in the local plasma properties, we followed Refs. [1,13] in making the assumption that oscillations in the pixel intensity at each location in the image plane scale with relative variations in the plasma density:

$$\tilde{I}(\boldsymbol{r}, t) \equiv \frac{I(\boldsymbol{r}, t) - \bar{I}(\boldsymbol{r})}{\bar{I}(\boldsymbol{r})} = \tilde{n}(\boldsymbol{r}, t) \equiv \frac{n(\boldsymbol{r}, t) - \bar{n}(\boldsymbol{r})}{\bar{n}(\boldsymbol{r})} \tag{1}$$

Here, $I(\boldsymbol{r}, t)$ and $n(\boldsymbol{r}, t)$ denote, respectively, the pixel intensity and density fluctuations at location $\boldsymbol{r}$ as a function of time t, and $\bar{I}(\boldsymbol{r})$ and $\bar{n}(\boldsymbol{r})$ are the time-averaged values. We note here that this relationship between pixel intensity and density is based on the implicit assumption that the electron temperature (which also influences light emission) is constant over the wave period. Although, as noted in previous studies [1,4,14], this assumption may be violated, the relative intensity of light emission can still provide insight into the local nature of perturbations in density.

III. Results

To investigate the properties of the fluctuations in the near field of the external cathode, we performed spectral analysis to examine the frequency content. amplitude, and phase analysis to characterize the dispersion. For our spectral analysis, we Fourier analyzed the time series $I_\omega(\boldsymbol{r}) = \mathcal{F}[\tilde{I}(\boldsymbol{r}, t)]$ from each pixel individually and then averaged over all the resulting power spectra $\langle |I_\omega(\boldsymbol{r})|^2 \rangle_r$. Figure 3c shows the averaged result, where the shaded region denotes the standard deviation from the average of the power spectra over pixels. We note here that the dominant source of uncertainty in these spectra is from the variation over pixels. We have neglected the error from the camera itself because these noise levels were $\sim$2%.

As shown in Fig. 3c, our analysis reveals two dominant frequency components in the near-field cathode region: a lower-amplitude mode at $8 \pm .9$ kHz, and a higher-amplitude mode at 56 ± 1 kHz, where we have estimated the error values by determining the peak frequency by randomly sampling values within the error bars (bootstrapping). The lower-frequency peak is associated with the so-called breathing mode, which is a ubiquitous longitudinal oscillation originating in the channel that has been observed on nearly all Hall thrusters [15–17]. The higher-frequency oscillation is within 20 kHz of the previously reported antidrift wave found in centrally mounted cathodes [1,3,8]. The observation of this frequency is our first correlational evidence that this localized cathode wave may persist even when the cathode is mounted externally.

Received 26 January 2021; revision received 18 June 2021; accepted for publication 20 June 2021; published online 5 August 2021.

*Ph.D. Candidate, Department of Aerospace Engineering, 1919 Green Road; shadrach@umich.edu. Student Member AIAA (Corresponding Author).

†Undergraduate Research Assistant, Department of Aerospace Engineering, 1919 Green Road.

‡Postdoctoral Fellow, Department of Aerospace Engineering, 1919 Green Road. Student Member AIAA.

§Assistant Professor, Department of Aerospace Engineering, 1320 Beal Avenue. Associate Fellow AIAA.

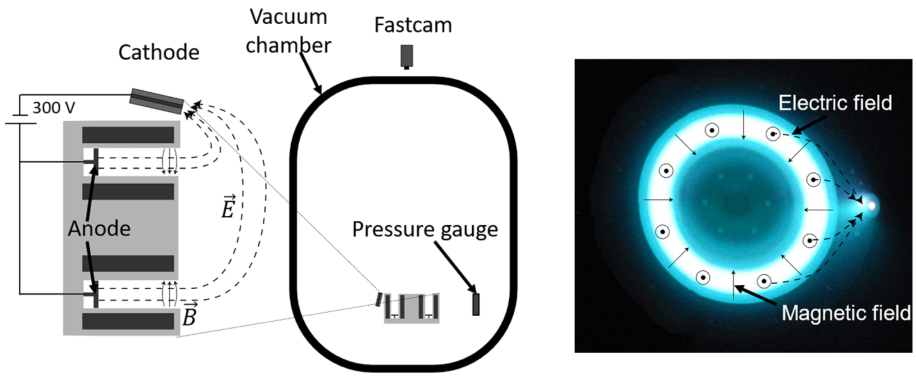

Fig. 1 Schematic and image of H9 Hall thruster operating at 300 V and 15 A with externally mounted cathode, with notional lines for magnetic and electric fields. Notional layout for experimental setup is also shown (not to scale).

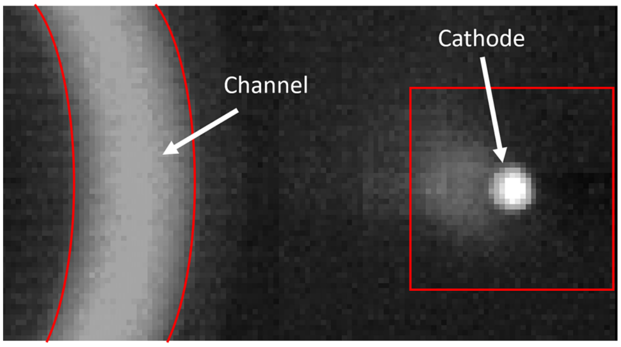

Fig. 2 Still image captured by high-speed camera. Red lines represent boundaries of channel (left) and pixels around cathode used in analysis (right).

To quantify the propagation of this higher-frequency wave and determine if it is in fact an azimuthal mode with respect to the cathode, we adopt the phase analysis methodology introduced in Ref. [1] and further implemented in Ref. [18]. To this end, we explicitly consider the Fourier expansion for the relative fluctuations at each pixel location:

$$\tilde{I}(\boldsymbol{r}, t) = \sum_{\omega} |I_{\omega}(\boldsymbol{r})| e^{i(-\omega t + \phi_{\omega}(\boldsymbol{r}))} \tag{2}$$

where $\phi_{\omega}(\boldsymbol{r})$ is the relative phase of the oscillation as a function of position. This term provides insight into the relative dispersion of the oscillations at frequency ω. We evaluate this phase by defining a reference pixel at location $\boldsymbol{r}_0$ with corresponding signal $\tilde{I}(\boldsymbol{r}_0, t)$ and phase $\phi_{\omega}(\boldsymbol{r}_0)$. We then perform a cross correlation between the signal intensity at this reference point $I(\boldsymbol{r}_0, t)$ and the other pixels in the image:

$$\Delta\phi_{\omega} = \phi_{\omega}(\boldsymbol{r}) - \phi_{\omega}(\boldsymbol{r}_0) = \tan^{-1}\left[\frac{\mathrm{Im}[I^*_{\omega}(\boldsymbol{r}_0) \cdot I_{\omega}(\boldsymbol{r})]}{Re[I^*_{\omega}(\boldsymbol{r}_0) \cdot I_{\omega}(\boldsymbol{r})]}\right] \tag{3}$$

Armed with this equation, we present in Fig. 3a the smoothed spatial map of the phase averaged over the frequency range 56 ± 1 kHz. In this figure, there is a gradual clockwise transition of phase from $-\pi$ to π in a circular pattern centered approximately on the cathode. This periodic transition in phase in the azimuthal direction suggests the observed oscillation is an $m = 1$ global mode propagating in a swirl around the cathode exit, i.e., that $\phi_{\omega}(\boldsymbol{r}) \approx m\theta$ in Eq. (2). Moreover, since the phase remains constant closer to the channel (left side of the image), our analysis suggests that the cathode mode has no dispersion in the channel. The dispersion of the wave at 56 kHz is thus local to the cathode: a result that is reminiscent of the phase analysis in figure 3b of Ref. [1], where the antidrift wave was first reported on a centrally mounted cathode. This indicates in turn that this mode is a distinct phenomenon from the previously reported "rotating spoke" mode, which propagates azimuthally but is confined to the main channel of the thruster [19]. We also note that the observed wave propagates in the diamagnetic direction. The magnetic field for our cathode is locally coaligned with the cathode axis while the pressure gradient is directed radially inward, toward the cathode axis. These two effects combine to lead to a local diamagnetic drift in the clockwise direction, which is consistent with the phase map shown in Fig. 3a. This direction of propagation aligns with previous work that has shown that the local antidrift oscillations in the cathode plume are driven unstable by this diamagnetic drift. The propagation direction thus provides additional correlational evidence that the mode with the external cathode is qualitatively similar to the waves observed in centrally mounted cathodes.

With that said, we do note a departure from this previous work. Although our oscillation evidently exhibits an azimuthal character, the axis of rotation appears to be centered at a point slightly below the cathode exit. On the other hand, in the previous study, the axis of rotation was collinear with the cathode axis. The underlying reason for this discrepancy may ultimately be attributed to the asymmetry of the external cathode configuration. We return to this point in the following section.

As a final assessment of this propagating mode, we show in Fig. 3b the two-dimensional spatial dependence of wave amplitude $|\tilde{I}_{\omega}(\boldsymbol{r})|^2$ at 56 kHz. We similarly show in Fig. 3d this amplitude as a function of radial position at four azimuthal locations. The dominant feature from these plots is the presence of an off-axis peak located on the side of the image closest to the thruster channel (to the left of the cathode orifice in the image). In contrast to the qualitative agreement in frequency and dispersion, this spatial distribution of the wave amplitude is a departure from previous studies on a centrally mounted cathode [1,8]. In this previous work, it was found that the azimuthal oscillation also exhibits an off-axis peak. However, this peak was azimuthally symmetric with respect to the cathode centerline. This is consistent with the hypothesis that the antidrift cathode wave is a nonlocal bulk oscillation. Our result instead shows the amplitude is preferentially peaked toward the thruster channel. With that said, the orientation of the camera with respect to the cathode precludes a direct comparison to previous results. Indeed, as shown in Fig. 1, the cathode exit is oriented at an angle with respect to the image plane. The image we generate is therefore a projection of the cathode plume onto this plane, which skews the integrated light intensity of oscillations. This skewing does not prevent us from detecting the overall rotation (as shown in Fig. 3a) but does preclude us from generating the same type of "face-on" assessment of the radial distribution of the plume amplitude that was done in previous studies. With that said, we do note that the relative magnitude of the spectrum of our oscillations is $\sim 0.2 \pm 0.1\%$ (see Fig. 3c), which is similar to the $\sim 1\%$ oscillations in luminosity reported in Ref. [1].

IV. Discussion

As we have outlined in the previous section, there are a number of correlational observations that suggests the external cathode also exhibits the same type of antidrift waves previously identified in Refs. [1,8], where thrusters with center-mounted cathodes were

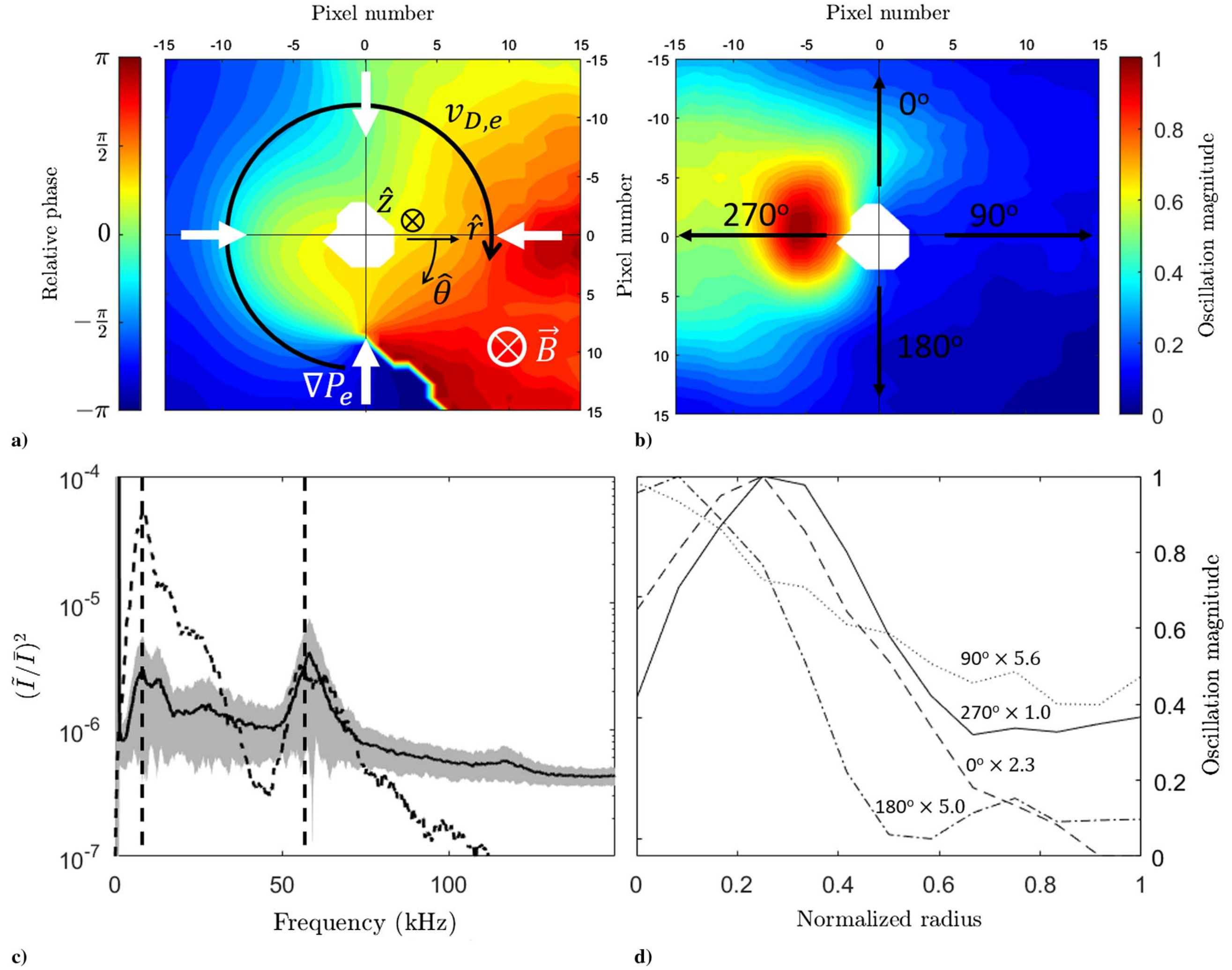

Fig. 3 Representations of a) phase plot, b) two-dimensional magnitude plot, c) power spectrum, and d) relative magnitude of the 56 kHz oscillation.

investigated. In particular, the frequency is comparable to previous findings (within 20 kHz), the wave is azimuthal with an $m = 1$ spatial distribution in the diamagnetic direction, and the amplitude is within an order of magnitude. To expand on this result, we can invoke the theory from Ref. [1] to be more quantitative in our comparison. This previous work presents a dispersion relation for an antidrift wave in a cathode plume invoking the full cylindrical geometry of the cathode. This dispersion relation is similar to that of Ellis et al. [20] in the limit of unmagnetized ions; and it is similar again to Ref. [8], which uses the dispersion relation in Cartesian coordinates. We expect the plasma parameters to be similar to those in Ref. [1], but the magnetic field is lower. We can thus replicate this analysis while assuming a magnetic field that is lower by a factor of 2.5. We follow the previous reference in allowing the parallel wave number to remain a free variable and assuming that the wave we observe will be the one with the highest growth rate. In doing so, we find that the most unstable mode exists at a parallel wave number of 25 m^{-1} with a real frequency of 60 kHz, which corresponds closely to what we observe.

Despite the fact that the external cathode is in a different position than the center-mounted cathodes from previous studies, the onset of this type of instability is not unexpected given the *local* similarities in the two plasma environments. Indeed, although the external cathode does not have overall symmetry with respect to the thruster axis, the plasma configuration is similar to the environment of a centrally mounted cathode in the vicinity of the cathode exit. Most notably, the magnetic field is approximately collinear with the axis of the cathode (shown qualitatively in Fig. 1); and since the plasma densities emerging from the cathode are the highest of any point in the thruster (cf. Ref. [8]), the local plasma properties and temperatures are dominated by this source. We therefore expect local symmetry with respect to the cathode axis, which is comparable in shape to the density profiles observed in previous work. This combination of the locally axial field and the radial gradients in the cathode plume promote the growth and propagation of the antidrift wave in the locally azimuthal direction.

With that said, although the theory and features of the measured wave agree qualitatively with previous results, we have remarked in Fig. 3a that the axis of rotation is slightly below the cathode centerline. This is a departure from previous results where the oscillation was observed to be centered on the orifice. As a possible explanation for this result, we note that the rotational mode will likely be anchored on the point of local symmetry (density, plasma potential, and temperature) of the cathode. Although we expect this point of symmetry to be close to the cathode orifice, it is plausible that with this external configuration, this anchor point is displaced by external forces. For example, as was noted in the work by Bourgeois et al. [21], the placement of the cathode can lead to asymmetric local drifts of the background plasma. Similarly, the strong Hall current (directed downward with respect to our image plane) also may convolve with the local cathode plume to shift the place of local symmetry downward. Ultimately, without a direct measurement of the local plasma properties, we cannot definitively explain this result. However, the fact that the center of rotation is displaced does not change the conclusion that the wave is locally rotational.

As a final comment, the existence of this antidrift wave on an external cathode suggests that it may have a similar impact on the local electron coupling environment as was found in Refs. [1,8]. For example, Ref. [8] hypothesized that the antidrift wave contributes to enhanced nonclassical cross-field transport in the cathode near field.

Given the similarity in the oscillation and its amplitude in the external configuration, we expect a similar effect may be anticipated for thrusters with external cathodes. This in turn suggests that just as with internally mounted cathodes, nonclassical effects must be considered to accurately represent the electrical coupling to the main discharge [22]. Similarly, it was also shown in Ref. [1] that this instability is correlated with fluctuations in the overall discharge current. The reason for this correlation was discussed at greater length in Ref. [8] and may in part be attributed to the fact that the antidrift wave exhibits a small but finite field-aligned component of propagation. To examine this correlation qualitatively in the present work, we show in Fig. 3c the power spectrum of the discharge current oscillations. As can be seen, the 56 kHz mode that is localized to the cathode is correlated with an oscillation in the discharge current. This is consistent with previous findings and indicates that this mode can and does impact the local electron dynamics. With that said, the discharge current oscillations are not one to one with the oscillations in the light intensity. This is not unexpected, however [1], given that the discharge current is a global measurement of all contributors to the current. The breathing mode ($\sim$8 kHz) traditionally has been the major source of oscillation in this parameter. The light intensity measurements, however, are only collected in the region we interrogated immediately adjacent to the cathode where the local antidrift mode induces an oscillation that has a larger amplitude than the breathing mode.

V. Conclusions

The goal of this Note has been to explore the possibility that an antidrift wave may exist in the near-field plume of a hollow cathode mounted in an external configuration for a HET. This work is motivated by previous studies that have shown this oscillation exists and can dominate the local dynamics for hollow cathodes mounted centrally on HETs. To this end, a combination of high-speed imaging and spatiotemporal Fourier analysis have been used to show that there is a mode that rotates locally around the cathode in a Hall thruster when its cathode is mounted in an external configuration. The properties of this wave (its $m = 1$ character, 56 kHz oscillation frequency, amplitude, and direction of propagation) suggest that this is the same type of antidrift wave that previously had been detected in hollow cathodes that were located on the thruster centerline.

Previous studies have shown that the cathode wave can contribute to variations in the overall discharge current of the thruster: both through promoting oscillations at the frequency of the wave as well as through enhancement of cross-field transport. The current work suggests that the same formalism and transport models that have emerged from previous studies on internal cathodes are relevant to external cathodes as well. It therefore may be critical to consider the impact of these modes to develop a self-consistent theory of the operation of an external cathode as well.

Acknowledgment

This work was funded under NASA Space Technology and Research Fellowship grant no. 80NSSC17K0156.

References

[1] Jorns, B. A., and Hofer, R. R., “Plasma Oscillations in a 6-kW Magnetically Shielded Hall Thruster,” *Physics of Plasmas*, Vol. 21, No. 5, 2014, Paper 053512.
https://doi.org/10.1063/1.4879819

[2] Jorns, B. A., Dodson, C., Goebel, D. M., and Wirz, R., “Propagation of Ion Acoustic Wave Energy in the Plume of a High-Current LaB6 Hollow Cathode,” *Physical Review E*, Vol. 96, No. 2, 2017, Paper 023208.
https://doi.org/10.1103/PhysRevE.96.023208

[3] Huang, W., Kamhawi, H., and Haag, T. W., “Plasma Oscillation Characterization of NASA’s HERMeS Hall Thruster via High Speed Imaging,” *52nd AIAA/SAE/ASEE Joint Propulsion Conference*, AIAA Paper 2016-4829, 2016.
https://doi.org/10.2514/6.2016-4829

[4] Georgin, M. P., Jorns, B. A., and Gallimore, A. D., “Correlation of Ion Acoustic Turbulence with Self-Organization in a Low-Temperature Plasma,” *Physics of Plasmas*, Vol. 26, No. 8, 2019, Paper 082308.
https://doi.org/10.1063/1.5111552

[5] Mikellides, I. G., and Katz, I., “Wear Mechanisms in Electron Sources for Ion Propulsion, 1: Neutralizer Hollow Cathode,” *Journal of Propulsion and Power*, Vol. 24, No. 4, 2008, pp. 855–865.
https://doi.org/10.2514/1.33461

[6] Mikellides, I. G., Katz, I., Goebel, D. M., and Jameson, K. K., “Evidence of Nonclassical Plasma Transport in Hollow Cathodes for Electric Propulsion,” *Journal of Applied Physics*, Vol. 101, No. 6, 2007, Paper 063301.
https://doi.org/10.1063/1.2710763

[7] Goebel, D. M., Jameson, K. K., Katz, I., and Mikellides, I. G., “Potential Fluctuations and Energetic Ion Production in Hollow Cathode Discharges,” *Physics of Plasmas*, Vol. 14, No. 10, 2007, Paper 103508.
https://doi.org/10.1063/1.2784460

[8] Jorns, B. A., Cusson, S. E., Brown, Z., and Dale, E., “Non-Classical Electron Transport in the Cathode Plume of a Hall Effect Thruster,” *Physics of Plasmas*, Vol. 27, No. 2, 2020, Paper 022311.
https://doi.org/10.1063/1.5130680

[9] Hofer, R. R., Cusson, S. E., Lobbia, R. B., and Gallimore, A. D., “The H9 Magnetically Shielded Hall Thruster,” *35th International Electric Propulsion Conference*, Electric Rocket Propulsion Soc. Paper IEPC-2017-232, Atlanta, GA, 2017, https://pepl.engin.umich.edu/pdf/IEPC-2017-232.pdf [retrieved 28 Oct. 2020].

[10] Cusson, S. E., Hofer, R. R., Lobbia, R., Jorns, B. A., and Gallimore, A. D., “Performance of the H9 Magnetically Shielded Hall Thrusters,” *International Electric Propulsion Conference*, Electric Rocket Propulsion Soc. Paper IEPC-2017-239, Atlanta, GA, 2017.

[11] Peterson, P. Y., Kamhawi, H., Huang, W., Yim, J., Herman, D., Williams, G., Gilland, J., and Hofer, R., “NASA HERMeS Hall Thruster Electrical Configuration Characterization,” *52nd AIAA/SAE/ASEE Joint Propulsion Conference*, AIAA Paper 2016-5027, 2016.

[12] Dankanich, J. W., Walker, M., Swiatek, M. W., and Yim, J. T., “Recommended Practice for Pressure Measurement and Calculation of Effective Pumping Speed in Electric Propulsion Testing,” *Journal of Propulsion and Power*, Vol. 33, No. 3, 2017, pp. 668–680.
https://doi.org/10.2514/1.B35478

[13] Sekerak, M. J., Longmier, B. W., Gallimore, A. D., Brown, D. L., Hofer, R. R., and Polk, J. E., “Azimuthal Spoke Propagation in Hall Effect Thrusters,” *IEEE Transactions on Plasma Science*, Vol. 43, No. 1, 2015, pp. 72–85.
https://doi.org/10.1109/TPS.2014.2355223

[14] Mcdonald, M. S., and Gallimore, A. D., “Rotating Spoke Instabilities in Hall Thrusters,” *IEEE Transactions on Plasma Science*, Vol. 39, No. 11, 2011, pp. 2952–2953.
https://doi.org/10.1109/TPS.2011.2161343.

[15] Lucca Fabris, A., Young, C. V., and Cappelli, M. A., “Time-Resolved Laser-Induced Fluorescence Measurement of Ion and Neutral Dynamics in a Hall Thruster During Ionization Oscillations,” *Journal of Applied Physics*, Vol. 118, No. 23, 2015, Paper 233301.
https://doi.org/10.1063/1.4937272

[16] Ito, T., Gascon, N., Crawford, W. S., and Cappelli, M. A., “Experimental Characterization of a Micro-Hall Thruster,” *Journal of Propulsion and Power*, Vol. 23, No. 5, 2007, pp. 1068–1074.
https://doi.org/10.2514/1.27140

[17] Young, C. V., Fabris, A. L., Macdonald-Tenenbaum, N. A., Hargus, W. A., and Cappelli, M. A., “Time-Resolved Laser-Induced Fluorescence Diagnostics for Electric Propulsion and their Application to Breathing Mode Dynamics,” *Plasma Sources Science and Technology*, Vol. 27, No. 9, 2018, Paper 094004.
https://doi.org/10.1088/1361-6595/aade42

[18] Romadanov, I., Raitses, Y., and Smolyakov, A., “Control of Coherent Structures via External Drive of the Breathing Mode,” *Plasma Physics Reports*, Vol. 45, No. 2, 2019, pp. 134–146.
https://doi.org/10.1134/S1063780X19020156

[19] Mcdonald, M. S., and Gallimore, A. D., “Parametric Investigation of the Rotating Spoke Instability in Hall Thrusters,” *32nd International Electric Propulsion Conference*, The Electric Rocket Propulsion Soc., Paper IEPC-2011-242, Wiesbaden, Germany, 2011, http://pepl.engin.umich.edu/pdf/IEPC-2011-242.pdf [retrieved 7 Oct. 2018].

[20] Ellis, R. F., Marden-Marshall, E., and Majeski, R., “Collisional Drift Instability of a Weakly Ionized Argon Plasma,” *Plasma Physics*, Vol. 22,

No. 2, 1980, pp. 113–131, https://iopscience.iop.org/article/10.1088/0032-1028/22/2/002/pdf [retrieved 2021].
https://doi.org/10.1088/0032-1028/22/2/002

[21] Bourgeois, G., Mazouffre, S., and Sadeghi, N., "Unexpected Transverse Velocity Component of Xe + Ions Near the Exit Plane of a Hall Thruster," *Physics of Plasmas*, Vol. 17, No. 11, 2010, Paper 113502.
https://doi.org/10.1063/1.3507308

[22] Jorns, B. A., and Byrne, M. P., "Model for the Dependence of Cathode Voltage in a Hall Thruster on Facility Pressure," *Plasma Sources Science and Technology*, Vol. 30, No. 1, 2021, Paper 015012.
https://doi.org/10.1088/1361-6595/abd3b6

Y. Ju
Associate Editor